International Journal of Engineering Technology and Management Sciences
Website: ijetms.in Issue:4 Volume No.10 July - August – 2026
DOI:10.46647/ijetms.2026.v10i04.004 ISSN: 2581-4621

A Multi-Model Time-Series Forecasting Framework for Food Crop Production and Sown Area in Vietnam, 2025-2030

Tong Thi Nhung[1*]
[1]*Faculty of Information Technology, Thuyloi University. 175 Tay Son - Kim Lien Ward - Hanoi City, Vietnam.*
**Correspondence: Tong Thi Nhung email: tongthinhung@tlu.edu.vn*

Abstract- Purpose: This study develops a forecasting framework for Vietnam's food crop production and sown area for 2025-2030. Methodology: Six time-series models - trend analysis, decomposition, moving average, single exponential smoothing, double exponential smoothing, and Holt-Winters - are benchmarked, with a proposed extension to feature screening and ensemble selection. Dataset: The empirical dataset is compiled from the 2024 Statistical Yearbook and contains two groups: ID 207, annual production of six annual crops (rice, maize, sugarcane, cassava, peanut, and sweet potato), and ID 209, food-grain sown area across six Vietnamese regions. Results: Across 12 series, the mean best MAPE is 1.375%; the lowest error is obtained for the Northern Midlands and Mountains area with MAPE = 0.14643%, while the most accurate production model is cassava with MAPE = 0.500%. Forecasts indicate sugarcane output may rise by 1,753.2 thousand tons (+13.96%), whereas peanut output may decline by 49.143 thousand tons (-12.61%) and Mekong Delta sown area may fall by 137.05 thousand hectares (-3.59%) by 2030. Value: The study provides an interpretable baseline for agricultural planning and shows how official statistics can be combined with future drone, camera, and sensor streams to support early warning, regional crop restructuring, and supply management.
Keywords- crop forecasting, food-grain sown area, Vietnam agriculture, time-series models, ensemble forecasting, precision agriculture

I. INTRODUCTION

Research object. Vietnamese agriculture remains a strategic sector for food security and rural livelihoods. This study focuses on two linked objects: crop production in ID 207 and food-grain sown area by region in ID 209. The production group covers rice, maize, sugarcane, cassava, peanut, and sweet potato, while the area group captures the Red River Delta, Northern Midlands and Mountains, North Central and Central Coast, Central Highlands, Southeast, and Mekong River Delta. Crop yield and production forecasting has become increasingly data-driven as machine learning, deep learning, and remote sensing make it possible to move from slow statistical reporting to proactive decision support [1]-[4].

Research gaps. Previous agricultural forecasting studies often emphasize one model family, one crop, or one spatial scale. Recent reviews show that Random Forest, gradient boosting, CNN, LSTM, and transformer models are widely used, yet they still depend on appropriate features, sufficient data length, and sensor availability [1], [2], [5], [6]. In Vietnam, a practical constraint is that official statistical series are reliable but usually annual and aggregated; therefore, they are useful for strategic forecasting but less capable of detecting within-season shocks. Drone and UAV studies also highlight high-resolution advantages, but cost, infrastructure, and operational readiness remain obstacles for small farms [7]-[9].

Research questions. The study answers three questions. RQ1: Which of the six time-series models gives the lowest error for each ID 207 and ID 209 series? RQ2: What are the forecasted 2025-2030 trends in crop production and regional food-grain area? RQ3: How can an official-statistics baseline be extended into a digital agriculture model using drone, camera, and sensor inputs?

Research value. The contribution is threefold. First, the study converts a Vietnamese course report into a publishable research structure using a transparent forecasting design. Second, it benchmarks six models and reports concrete errors and forecasts. Third, it bridges classical time-series

DOI:10.46647/ijetms.2026.v10i04.004 ISSN: 2581-4621

forecasting with the precision-agriculture literature, where multispectral UAV imagery, crop growth models, and multi-modal deep ensembles are increasingly important [3], [5], [8]-[10].

Research objectives. The objectives are to compile and describe the ID 207 and ID 209 datasets, evaluate the candidate models by MAPE, MAD, and MSD, select the best-performing model for each series, produce 2025-2030 forecasts, and discuss policy implications through a SWOT framework.

Paper organization. Section II reviews related literature. Section III presents the proposed research model and mathematical formulation. Section IV reports empirical results. Section V discusses the findings using SWOT and comparison with prior studies. Section VI concludes the paper and proposes future research directions.

II. RELATED LITERATURE REVIEW

A. Classical and statistical forecasting

Manual crop forecasting relies on field reports, local officer observations, and farmer declarations. It is inexpensive and easy to deploy but is slow, subjective, and weak in detecting short-term changes in pests, floods, drought, or crop density. Statistical time-series methods address part of this problem by modeling trend, level, smoothing, and seasonality, but annual aggregate data still constrain their ability to represent field-level dynamics.

Recent computational reviews emphasize that rice and grain yield forecasting requires careful dataset construction, preprocessing, feature selection, and model validation [11], [12]. In rice-specific studies, the major challenge is to represent phenology, soil background, climate variability, and spatial heterogeneity. Such evidence supports the use of a transparent baseline for Vietnam before introducing higher-frequency sensor streams.

B. Machine learning, deep learning, and remote sensing

Machine learning studies demonstrate the value of satellite and climate variables. District-level rice prediction using climate reanalysis and remote sensing achieved strong out-of-sample performance, with reported R2 up to 0.82 and MAPE around 0.16 in one benchmark [12]. SAR and optical remote sensing combined with biophysical parameters have also improved early-stage rice yield prediction [13].

Deep reinforcement learning and multi-source remote sensing have been proposed to integrate historical yields, weather, soil, and satellite imagery, reporting high model accuracy in crop forecasting tasks [14]. IoT-based approaches such as the Crop Yield Prediction Algorithm incorporate climate, weather, chemicals, and agricultural variables and achieved model scores above 0.99 for tree-based regressors in one study [15]. These results suggest that Vietnam's annual-statistics baseline should eventually be expanded to weather, soil, image, and sensor data.

C. Feature selection and ensemble learning

Feature selection remains central to robust crop prediction. Hybrid feature-selection frameworks using correlation filters, information gain, recursive feature elimination, and optimized support vector regression show that reducing irrelevant variables can improve generalization and computational efficiency [16]. Gradient-based machine learning methods such as CatBoost, LightGBM, and XGBoost have also produced high reported accuracy in crop yield tasks [17].

Deep learning review work shows that CNN and LSTM architectures dominate applied crop yield prediction, especially when satellite imagery or UAV data are available [18]. More recent multi-site maize prediction studies combine agronomic traits and meteorological data to improve generalizability under climate uncertainty [19]. Reviews of remote sensing-based crop yield estimation argue that future systems should combine optical, SAR, UAV, crop-simulation, and machine learning methods for scalable monitoring [20]. The proposed framework in this paper follows that direction but begins with a concise, interpretable time-series baseline.

International Journal of Engineering Technology and Management Sciences
Website: ijetms.in Issue:4 Volume No.10 July - August – 2026
DOI:10.46647/ijetms.2026.v10i04.004 ISSN: 2581-4621

III. PROPOSED RESEARCH MODEL AND METHODOLOGY

The proposed model contains five stages: database construction, feature screening, candidate forecasting, ensemble/model selection, and policy output (Figure 1). The first implementation uses annual ID 207 and ID 209 statistical series. The model is designed so that future images from drones or smart cameras and measurements from environmental sensors can be added as external features without changing the forecasting logic.

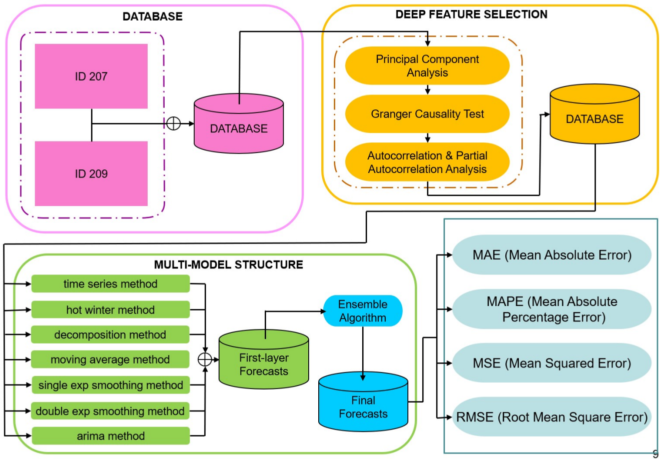

Fig. 1. Proposed data-driven forecasting framework.

Step 1. Database construction

The cleaned dataset is denoted as $D=\{(i,t,y_{i,t}),\mid i=1,\ldots 12\ t=2015\ldots 2024\}$, where $y_{i,t}$ represents the annual observation of series i in year t. Among the 12 series, ID 207 records production measured in thousand tons, while ID 209 represents harvested area measured in thousand hectares. The remaining series are organized in the same annual format according to their respective units. This dataset serves as the foundation for the forecasting framework. In future extensions, the dataset can be enriched by incorporating exogenous variables $x_{i,t}$, such as the Normalized Difference Vegetation Index (NDVI), rainfall, temperature, humidity, and UAV-derived vegetation indices, to improve model performance and capture the influence of environmental conditions on agricultural production.

Table 1. Dataset structure used in the study

Group	Series	Unit
ID 207	Rice, maize, sugarcane, cassava, peanut, sweet potato production	Thousand tons
ID 209	Food-grain sown area in six Vietnamese regions	Thousand hectares

Step 2. Feature screening and statistical diagnosis

Feature selection is applied to future multi-source datasets to remove redundant variables and improve forecasting performance. First, the linear relationship between variables is measured using the Pearson correlation coefficient, $r_{xy}=\frac{\sum_t (x_t-\bar{x})(y_t-\bar{y})}{\sqrt{\sum_t (x_t-\bar{x})^2 \sum_t (y_t-\bar{y})^2}}$, which identifies highly correlated features that may provide overlapping information. Multicollinearity is then assessed using the Variance Inflation Factor (VIF), $\mathrm{VIF}_j=\frac{1}{1-R_j^2}$, where R_j^2 is obtained by regressing feature j on the remaining features. To reduce dimensionality while preserving most of the data variance, Principal Component Analysis (PCA) ranks transformed components according to their explained variance ratio, $\mathrm{EVR}_j=\frac{\lambda_j}{\sum_k \lambda_k}$,
where λ_j denotes the eigenvalue of the j-th principal component. Analysis of Variance (ANOVA) is further employed to evaluate the statistical significance of group differences using the F-statistic, $F=\frac{MS_{\text{between}}}{MS_{\text{within}}}$, where MS_{between} and MS_{within} represent the between-group and within-group mean

International Journal of Engineering Technology and Management Sciences
Website: ijetms.in Issue:4 Volume No.10 July - August – 2026
DOI:10.46647/ijetms.2026.v10i04.004 ISSN: 2581-4621

squares, respectively. Finally, the Least Absolute Shrinkage and Selection Operator (LASSO) is used to eliminate weak predictors by minimizing the objective function $\min_{\beta}\left\{\frac{1}{2n}\sum_{t=1}^{n}(y_t-x_t\beta)^2+\lambda\,/\!/\,\beta\,/\!/_1\right\}$, which simultaneously performs variable selection and regularization, thereby retaining the most informative features for the forecasting model.

Step 3. Candidate forecasting models

Classical statistical forecasting methods are employed as baseline models to capture different patterns in the time series. The simplest approach is trend regression, which assumes a linear relationship between the observation and time, expressed as $y_t=\beta_0+\beta_1 t+\varepsilon_t$, where β_0 and β_1 are the regression coefficients and ε_t is the random error term. Future values are forecast using $\hat{y}_{t+\mathrm{h}}=\beta_0+\beta_1(t+\mathrm{h})$. For series exhibiting multiple structural components, the decomposition model represents the observations as the sum of trend, seasonal, and irregular components, $y_t=T_t+S_t+I_t$, under an additive decomposition framework. A simple smoothing alternative is the moving average method, which forecasts the next observation as the average of the most recent k observations, $F_{t+1}=\frac{1}{k}\sum_{j=0}^{k-1} y_{t-j}$. Another widely used approach is single exponential smoothing, which assigns exponentially decreasing weights to historical observations according to $F_{t+1}=\alpha y_t+(1-\alpha)F_t$, $0<\alpha<1$. For time series with a trend component, Holt's exponential smoothing extends this formulation by updating both the level and trend, $l_t=\alpha y_t+(1-\alpha)(l_{t-1}+b_{t-1})$, $b_t=\beta(l_t-l_{t-1})+(1-\beta)b_{t-1}$, with future forecasts computed as $\hat{y}_{t+\mathrm{h}}=l_t+\mathrm{h}b_t$. When both trend and seasonality are present, the Holt–Winters method further incorporates a seasonal component, producing forecasts of the form $\hat{y}_{t+\mathrm{h}}=l_t+\mathrm{h}b_t+s_{t+\mathrm{h}-m}$, where m denotes the seasonal period. For more complex temporal dependencies, the AutoRegressive Integrated Moving Average (ARIMA) model is adopted, which combines autoregressive, differencing, and moving-average components. The general ARIMA formulation is $\phi(B)(1-B)^d y_t=\theta(B)\varepsilon_t$, where B is the backshift operator, d is the order of differencing, and $\phi(B)$ and $\theta(B)$ are the autoregressive and moving-average polynomials, respectively. These classical methods provide interpretable baselines for comparison with more advanced machine learning and deep learning forecasting models.

Step 4. Ensemble and error-based model selection

Each forecasting model m produces a first-layer prediction, denoted by $\hat{y}_{m,t+\mathrm{h}}$. When multiple forecasting models are available, their outputs can be combined through an ensemble approach to improve predictive performance. The ensemble forecast is calculated as $\hat{y}_{t+\mathrm{h}}=\sum_{m=1}^{M} w_m\,\hat{y}_{m,t+\mathrm{h}}$, where $w_m\geq 0$ represents the weight assigned to model m, subject to the constraint $\sum_{m=1}^{M} w_m=1$. A common weighting strategy is inverse-error weighting, in which models with lower validation errors receive higher weights. The weights are computed as $w_m=\frac{1/E_m}{\sum_j(1/E_j)}$, where E_m is the validation error of model m, typically measured using the Mean Absolute Percentage Error (MAPE) or the Root Mean Squared Error (RMSE). In the present empirical implementation, however, no ensemble is constructed; instead, the forecasting model with the lowest validation MAPE is selected as the final model for each individual time series.

Forecasting performance is evaluated using several widely adopted accuracy metrics. The Mean Absolute Error (MAE) measures the average magnitude of prediction errors and is defined as $\mathrm{MAE}=\frac{1}{n}\sum_{t=1}^{n}|y_t-\hat{y}_t|$. The Mean Absolute Percentage Error (MAPE) expresses the average prediction error as a percentage of the observed values, $\mathrm{MAPE}=\frac{100}{n}\sum_{t=1}^{n}\left|\frac{y_t-\hat{y}_t}{y_t}\right|$. The Mean Squared Error (MSE) evaluates forecasting performance by averaging the squared prediction errors, while the Root Mean Squared Error (RMSE) is obtained as $\mathrm{RMSE}=\sqrt{\mathrm{MSE}}$, providing an error measure in the same unit as the original observations. Although the original report refers to the Mean Squared Deviation (MSD), this study treats MSD as the squared-deviation criterion equivalent to MSE and

International Journal of Engineering Technology and Management Sciences
Website: ijetms.in Issue:4 Volume No.10 July - August – 2026
DOI:10.46647/ijetms.2026.v10i04.004 ISSN: 2581-4621

reports it alongside MAE and MAPE to provide a comprehensive assessment of forecasting accuracy.

IV. RESEARCH RESULTS

A. Descriptive statistics

The dataset shows stable behavior in some crops and high dispersion in others. For example, rice production ranges from 42,661 to 43,853 thousand tons with sigma = 512, while sweet potato production ranges from 914.7 to 1,378 thousand tons with sigma = 200.1. Regional area is largest in the Mekong River Delta, with a maximum of 3,991.2 thousand hectares and sigma = 62.5.

Table 2. Descriptive statistics of ID 207 and ID 209 series

ID	Content	Max	Min	Mean	Sigma
ID 207-1	Rice production	43,853	42,661	43,246	512
ID 207-2	Maize production	4,558.2	4,402.2	4,453.5	60.9
ID 207-3	Sugarcane production	12,675	10,741	11,577	744
ID 207-4	Cassava production	10,627	10,439	10,534	69.8
ID 207-5	Peanut production	430.4	397.2	412.26	14.96
ID 207-6	Sweet potato production	1,378	914.7	1,094.7	200.1
ID 209-1	Red River Delta sown area	1,047.8	985.2	1,014.1	25.8
ID 209-2	Northern midlands and mountains area	1,092.4	1,047.5	1,068.3	17.3
ID 209-3	North Central and Central Coast area	1,375.1	1,331.2	1,156.0	15.8
ID 209-4	Central Highlands area	439.7	418.8	426.0	8.03
ID 209-5	Southeast area	320.3	306.4	310.84	6.04
ID 209-6	Mekong River Delta area	3,991.2	3,827.7	3,897.9	62.5

B. Model performance

The best model varies by series. Trend Analysis is selected for five series, Decomposition for four series, Single Smoothing for two series, and Moving Average for one series. The average best MAPE across the 12 series is 1.375%. Across all six candidate models, the average MAPE is 1.514% for Trend Analysis, 1.554% for Decomposition, 1.714% for Single Smoothing, 1.889% for Holt-Winters, 2.939% for Double Smoothing, and 3.356% for Moving Average.

Table 3. Best-performing model by series

ID	Crop/region	Selected model	MAPE (%)	MAD	MSD
ID 207-1	Rice	Decomposition	0.600	247.2	74,861.4
ID 207-2	Maize	Trend Analysis	0.621	27.736	900.994
ID 207-3	Sugarcane	Trend/Decomp./Single	4.000	405-487	202,725-268,635

International Journal of Engineering Technology and Management Sciences
Website: ijetms.in Issue:4 Volume No.10 July - August – 2026
DOI:10.46647/ijetms.2026.v10i04.004 ISSN: 2581-4621

ID 207-4	Cassava	Trend Analysis	0.500	52.5	3,811.56
ID 207-5	Peanut	Decomposition	1.0064	4.1225	21.8334
ID 207-6	Sweet potato	Single Smoothing	6.590	72.71	8,521.8
ID 209-1	Red River Delta	Decomposition	0.20235	2.02949	5.07995
ID 209-2	Northern midlands and mountains	Trend Analysis	0.14643	1.572	2.8774
ID 209-3	North Central & Central Coast	Moving Average	0.5032	6.8333	58.125
ID 209-4	Central Highlands	Decomposition	0.9255	3.9618	20.2816
ID 209-5	Southeast	Single Smoothing	0.58603	1.83038	7.99788
ID 209-6	Mekong River Delta	Trend Analysis	0.820	31.7	1,623.66

C. Forecasts for 2025-2030

The 2025-2030 forecasts indicate divergence between crop groups. Sugarcane has the strongest positive outlook, increasing from 12,555.1 to 14,308.3 thousand tons. In contrast, peanut production decreases from 389.787 to 340.644 thousand tons, a decline of 12.61%. Rice and maize both decline, while cassava remains nearly stable. The sown area of the Red River Delta, Northern Midlands and Mountains, Central Highlands, and Mekong River Delta decreases, while the North Central and Central Coast and Southeast series remain almost stable.

Table 4. Forecasted changes for 2025-2030

ID	Indicator	Forecast range	Change	%
ID 207-1	Rice production	44,104.5 -> 43,704.8 thousand tons	-399.7	-0.91%
ID 207-2	Maize production	4,357.1 -> 4,196.5 thousand tons	-160.6	-3.69%
ID 207-3	Sugarcane production	12,555.1 -> 14,308.3 thousand tons	+1,753.2	+13.96%
ID 207-4	Cassava production	10,513.9 -> 10,480.5 thousand tons	-33.4	-0.32%
ID 207-5	Peanut production	389.787 -> 340.644 thousand tons	-49.143	-12.61%
ID 207-6	Sweet potato production	2024 level 972.9 -> 2030 level 1,001.62 thousand tons	+28.72	+2.95%
ID 209-1	Red River Delta area	964.52 -> 884.745 thousand ha	-79.775	-8.27%
ID 209-2	Northern midlands and mountains area	1,035.65 -> 981.20 thousand ha	-54.45	-5.26%
ID 209-3	North Central & Central Coast area	Approx. 1,356.6 thousand ha	Stable	0.00%
ID 209-4	Central Highlands area	414.083 -> 394.549 thousand ha	-19.534	-4.72%
ID 209-5	Southeast area	Approx. 307.398 thousand ha	Stable	0.00%
ID	Mekong River	3,815.65 -> 3,678.60 thousand ha	-137.05	-3.59%

International Journal of Engineering Technology and Management Sciences
Website: ijetms.in Issue:4 Volume No.10 July - August – 2026
DOI:10.46647/ijetms.2026.v10i04.004 ISSN: 2581-4621

209-6	Delta area			

D. Main empirical findings

Finding 1: the area series are easier to forecast than some production series. The smallest MAPE is 0.14643% for ID 209-2, followed by 0.20235% for ID 209-1. Finding 2: among production series, cassava and rice are stable, with best MAPEs of 0.500% and 0.600%, respectively. Finding 3: sweet potato is the most difficult series, with best MAPE = 6.590%, reflecting larger historical volatility. Finding 4: the most relevant policy warning concerns the simultaneous decline in peanut output (-12.61%) and major regional area contraction in the Red River Delta (-8.27%) and Mekong River Delta (-3.59%).

V. SWOT-BASED DISCUSSION

Compared with recent machine learning and remote sensing studies, this paper is intentionally more interpretable and data-light. Transformer and UAV-image models can capture within-season crop signals and reduce prediction error in image-rich settings [3], [9], while multi-source deep ensembles can improve regional rice yield prediction when SAR, optical, and meteorological variables are available [10], [13]. The advantage of the present approach is that it can be implemented immediately from official statistical series and can produce transparent policy-level forecasts. Its limitation is the absence of in-season crop condition variables.

Table 5. SWOT comparison of the proposed study

SWOT element	Interpretation
Strengths	Uses two complementary data groups, benchmarks six models, reports concrete errors and 2030 forecasts, and gives transparent results suitable for policy discussion.
Weaknesses	Annual data are short, direct yield series are unavailable, and the drone/camera/sensor architecture is proposed rather than fully populated with long-term data.
Opportunities	Can be expanded with UAV multispectral images, smart-camera crop status, soil moisture, rainfall, temperature, and online dashboards for early warning.
Threats	Climate shocks, salinity in the Mekong Delta, urbanization in the Red River Delta, high device cost, and uneven rural digital infrastructure may reduce forecasting accuracy and adoption.

The SWOT analysis suggests that the model should not be interpreted as a replacement for field inspection or remote sensing. Instead, it is a strategic baseline that can identify series needing attention. For example, the strong sugarcane increase (+13.96%) implies potential value-chain expansion, whereas the peanut decline (-12.61%) suggests a need to examine area conversion, seed quality, irrigation, and market incentives. The Mekong Delta area contraction (-137.05 thousand hectares) is consistent with the need to manage salinity and crop restructuring risks.

VI. CONCLUSION

This study contributes a structured IJETMS-style research article and a multi-model forecasting framework for Vietnam's food crop production and food-grain sown area. Its practical value is the transformation of annual statistical data into actionable forecasts for crop planning, regional restructuring, and supply management. Its academic value is the integration of classical time-series benchmarking with an extensible precision-agriculture architecture.

The empirical results are specific. The mean best MAPE over 12 series is 1.375%. ID 209-2 has the lowest MAPE at 0.14643%, and ID 207-4 has the lowest production MAPE at 0.500%. Forecasts show sugarcane increasing by 1,753.2 thousand tons (+13.96%), peanut decreasing by 49.143 thousand tons (-12.61%), rice decreasing by 399.7 thousand tons (-0.91%), maize decreasing by 160.6 thousand tons (-3.69%), and the Mekong Delta area decreasing by 137.05 thousand hectares (-3.59%) by 2030.

The limitations are clear. The official annual dataset is short, and direct yield observations are not separated from production and area in the available tables. Drone, camera, and sensor data are proposed as part of the architecture, but long-term field-level data are not yet available for validation. In addition, unexpected shocks such as pests, extreme rainfall, drought, salinity, and market shifts may reduce the reliability of purely historical forecasts.

Future research should collect longer regional crop panels, integrate Sentinel-1/2 imagery and UAV multispectral images, add soil and climate variables, test ARIMA, Prophet, gradient boosting, LSTM, and transformer baselines, and deploy an online dashboard for farmers and local authorities. The next stage should also estimate direct productivity indicators by combining production and area, thereby distinguishing output growth driven by yield improvement from output growth driven by area expansion.

Acknowledgments: The authors thank Thuyloi University, Vietnam, for academic guidance and support.

REFERENCES

[1] M. A. Jabed and M. A. A. Murad, "Crop yield prediction in agriculture: A comprehensive review of machine learning and deep learning approaches, with insights for future research and sustainability," Heliyon, vol. 10, 2024, doi: 10.1016/j.heliyon.2024.e40836.

[2] S. M. Shawon, F. B. Ema, A. K. Mahi, F. L. Niha, and H. T. Zubair, "Crop yield prediction using machine learning: An extensive and systematic literature review," Smart Agricultural Technology, 2024, doi: 10.1016/j.atech.2024.100718.

[3] L. Bi, O. Wally, G. Hu, A. U. Tenuta, Y. R. Kandel, and D. S. Mueller, "A transformer-based approach for early prediction of soybean yield using time-series images," Frontiers in Plant Science, vol. 14, 2023, doi: 10.3389/fpls.2023.1173036.

[4] Y. Sadeh, X. Zhu, D. Dunkerley, J. P. Walker, Y. Chen, and K. Chenu, "Versatile crop yield estimator," Agronomy for Sustainable Development, vol. 44, no. 42, 2024, doi: 10.1007/s13593-024-00974-4.

[5] H. Zhou, F. Huang, W. Lou, Q. Gu, Z. Ye, H. Hu, and X. Zhang, "Yield prediction through UAV-based multispectral imaging and deep learning in rice breeding trials," Agricultural Systems, 2024, doi: 10.1016/j.agsy.2024.104214.

[6] D. De Clercq and A. Mahdi, "Modern computational approaches for rice yield prediction: A systematic review of statistical and machine learning-based methods," Computers and Electronics in Agriculture, vol. 231, 2025, doi: 10.1016/j.compag.2024.109852.

[7] H. Zhu, C. Lin, G. Liu, D. Wang, S. Qin, A. Li, J.-L. Xu, and Y. He, "Intelligent agriculture: deep learning in UAV-based remote sensing imagery for crop diseases and pests detection," Frontiers in Plant Science, vol. 15, 2024, doi: 10.3389/fpls.2024.1435016.

[8] R. Guebsi, S. Mami, and K. Chokmani, "Drones in precision agriculture: A comprehensive review of applications, technologies, and challenges," Drones, vol. 8, no. 11, p. 686, 2024, doi: 10.3390/drones8110686.

[9] J. Yuan, Y. Zhang, Z. Zheng, W. Yao, W. Wang, and L. Guo, "Grain crop yield prediction using machine learning based on UAV remote sensing: A systematic literature review," Drones, vol. 8, no. 10, p. 559, 2024, doi: 10.3390/drones8100559.

[10] A. D. Yewle, L. Mirzayeva, and O. Karakus, "Multi-modal data fusion and deep ensemble learning for accurate crop yield prediction," Remote Sensing Applications: Society and Environment, 2025, doi: 10.1016/j.rsase.2025.101613.

[11] G. S. Mmbando, "Harnessing artificial intelligence and remote sensing in climate-smart agriculture: the current strategies needed for enhancing global food security," Cogent Food & Agriculture, 2025, doi: 10.1080/23311932.2025.2454354.

[12] D. De Clercq and A. Mahdi, "Feasibility of machine learning-based rice yield prediction in India at the district level using climate reanalysis and remote sensing data," Agricultural Systems, vol. 220, p. 104099, 2024, doi: 10.1016/j.agsy.2024.104099.

DOI:10.46647/ijetms.2026.v10i04.004 ISSN: 2581-4621

[13] S. Sah, D. Haldar, R. N. Singh, B. Das, and A. S. Nain, "Rice yield prediction through integration of biophysical parameters with SAR and optical remote sensing data using machine learning models," Scientific Reports, vol. 14, 2024, doi: 10.1038/s41598-024-72624-4.
[14] Y. R. Chavan, B. Swamikan, M. V. Gupta, S. Bobade, and A. Malhan, "Enhanced crop yield forecasting using deep reinforcement learning and multi-source remote sensing data," Remote Sensing in Earth Systems Sciences, vol. 7, pp. 426-442, 2024, doi: 10.1007/s41976-024-00135-x.
[15] F. M. Talaat, "Crop yield prediction algorithm (CYPA) in precision agriculture based on IoT techniques and climate changes," Neural Computing and Applications, vol. 35, pp. 17281-17292, 2023, doi: 10.1007/s00521-023-08619-5.
[16] M. Abdel-salam, N. Kumar, and S. Mahajan, "A proposed framework for crop yield prediction using hybrid feature selection approach and optimized machine learning," Neural Computing and Applications, vol. 36, pp. 20723-20750, 2024, doi: 10.1007/s00521-024-10226-x.
[17] P. Mahesh and R. Soundrapandiyan, "Yield prediction for crops by gradient-based algorithms," PLOS ONE, vol. 19, no. 8, e0291928, 2024, doi: 10.1371/journal.pone.0291928.
[18] K. Meghraoui, I. Sebari, J. Pilz, K. Ait El Kadi, and S. Bensiali, "Applied deep learning-based crop yield prediction: A systematic analysis of current developments and potential challenges," Technologies, vol. 12, no. 4, p. 43, 2024, doi: 10.3390/technologies12040043.
[19] C. Ma, Z. Ye, Q. Zi, and C. Liu, "Machine-learning-based multi-site corn yield prediction integrating agronomic and meteorological data," Agronomy, vol. 15, no. 8, p. 1978, 2025, doi: 10.3390/agronomy15081978.
[20] A. Muhammad, A. S. Mashori, M. Jan, Z. Han, F. Li, S. Jan, and S. A. Shah, "A review of remote sensing-based crop yield estimation: machine learning, deep learning, and crop growth models," Frontiers in Plant Science, 2026, doi: 10.3389/fpls.2026.1742689.